

303168

**SIMULATIONS OF ISOPRENE - OZONE REACTIONS  
FOR A  
GENERAL CIRCULATION/CHEMICAL TRANSPORT MODEL**

*P. A. Makar and J.C. McConnell*  
CRESS, York University, Toronto, Canada, M3J 1P3

**Abstract:**

A parameterized reaction mechanism has been created to examine the interactions between isoprene and other tropospheric gas-phase chemicals. Tests of the parameterization have shown that its results match those of a more complex reaction set to a high degree of accuracy. Comparisons between test runs have shown that the presence of isoprene at the start of a six day interval can enhance later ozone concentrations by as much as twenty-nine percent. The test cases used no input fluxes beyond the initial time, implying that a single input of a biogenic hydrocarbon to an airmass can alter its ozone chemistry over a time scale on the order of a week.

**Introduction:**

Various studies (cf. Jacob and Wofsy, 1988, Trainer et al., 1987) have suggested that fluxes of terpenes such as isoprene may be responsible for enhanced ozone concentrations in the lower troposphere. The full reaction mechanisms for these gases are too complex for use in chemical transport models, due to the memory space required to store all species, and the computation time needed to predict future concentrations. The present work discusses the parameterization of one of these mechanisms (that of isoprene) into a simplified form. The effect of an initial input of isoprene on later ozone chemistry was studied as part of the parameterization process.

**Constructing the Parameterization.**

In the following discussion, reference will be made to three reaction sets; "no isoprene", "parameterization" and "full isoprene". The first is a simplified tropospheric reaction set, following Lurmann et al. (1986) and DeMore et al. (1990). The "full isoprene" set includes the no isoprene reactions and the detailed isoprene system of Lurmann et al. (1986), and incorporates some of the changes suggested by Jacob and Wofsy (1988). The "parameterization" is the simplified isoprene mechanism, designed to have the same effect on the simple troposphere as the full isoprene set, yet using fewer species to accomplish this goal. The parameterized reaction mechanism and its rates are given in Appendix I.

The parameterization was constructed by eliminating unimportant reaction pathways and lumping species with similar chemistry together. In summary, the changes were:

(1) Criegee - type radicals MVKO, MAOO, and MCRG were lumped together as "CREB". The products of the oxidation of CREB by NO were determined by adding the three oxidation reactions of CREB's components.

(2) Radicals  $MAN_2$  and  $MVN_2$  (produced via  $NO_3$  oxidation of methacrolein and methyl vinyl ketone, respectively) were lumped together as " $MBN_2$ ". The

product coefficients for the subsequent reaction of  $MBN_2$  with NO were derived by examining the amount of  $MBN_2$  resulting from each of the methacrolein and methyl vinyl ketone paths.

(3) Radicals  $MRO_2$  and  $VRO_2$  (produced via OH reactions with MACR and MVK, respectively) were lumped together as " $BRO_2$ ", with product species and reaction coefficients adjusted as in step (2).

(4) The cycles for the natural acetyl nitrate species IPAN and MPAN were lumped together into the PAN cycle. The products leaving the cycle via oxidation of the lumped carbonate by NO are dependant on the concentrations of MACR and MVK. With this change,  $CH_3CHO$  and  $HOCH_2CHO$  are lumped as a single higher aldehyde,  $CH_3CO_3$  and  $MAO_3$  are similarly lumped, and the total acetyl-nitrate is the sum of PAN, IPAN, and MPAN concentrations. The reaction rates used were those of the normal PAN cycle, but the products and their coefficients were changed to reflect the new sources of total PAN.

(5) Product species  $IPN_4$ , MGLO, pyruvic acid and methyl acrylic acid were dropped from the parameterization, as were the reactions for the production of ozonides.

**Numerical Tests of the Parameterization:**

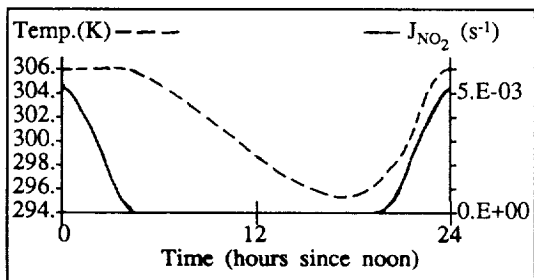
Nine test simulations were performed, each simulation spanning six days of diurnally varying photochemistry. No fluxes or deposition were allowed after the initial start-up of the box model. The initial conditions for these tests are given in Table 1. Most of the chemicals had the same initial concentration regardless of the test. The only species with different concentrations at the initial time were  $NO_2$ , NO,  $O_3$ , PAN, and isoprene.  $NO_x$ , ozone and PAN started at three levels, representing background, rural and polluted urban air. Isoprene was set at three levels. The combinations of the three  $NO_x$  scenarios with the three isoprene levels resulted in the nine test cases. Similarly, the level of  $NO_x$  and isoprene are the only possible causes of the differences between the simulations.

Reaction rates were calculated assuming sea-level pressures at the equator close to equinox. Photochemical rates were calculated using a detailed one-dimensional model (Henderson et al., 1987). The diurnal temperature profile and an example photochemical rate are given in Figure 1.

Simulations began at noon on the first day, with the noon-to-noon diurnal profile in rates repeating during the subsequent five days.

Two types of analysis were made with the resulting data. The effect of isoprene reactions on the model atmosphere were shown by comparing no isoprene and full isoprene simulations. The parameterization results were compared to the full isoprene results in order to gauge the usefulness of the former in simulating isoprene chemistry.

Figure 1. Temperature profile and  $J_{NO_2}$ .



Only a few species will be shown and discussed, due to the large amount of data resulting from these simulations and the limited space for this presentation. Researchers interested in obtaining the data files or plots of the results should contact the authors at the above address.

The  $O_3$  results for each test are given in Fig. 2. Each graph shows the concentrations (ppbv) as functions of time, and are labeled according to the initial concentration scenario giving rise to the data. As can be seen from the graphs, the ozone concentration is enhanced by the addition of isoprene if the initial  $NO_x$  level is high or medium, and is depleted if the initial  $NO_x$  is low. The largest  $O_3$  increase is for the case (high initial  $NO_x$ , high initial isoprene), in which the ozone maximum is 25 ppbv higher after the addition of isoprene (maximum of 83.8 ppbv without isoprene, and

108.3 ppbv with initial isoprene), an enhancement of 29%. The parameterization's  $O_3$  values were within a few percent of those from the full isoprene mechanism for all test runs. The parameterization would appear to be suitable for  $O_3$  simulations, with the caveat that ozone may be overpredicted by up to 5 ppbv.

The cause of the  $O_3$  enhancements are explained via the relative steady state between  $O_3$  and  $NO_x$ . Steady state ozone concentrations are roughly proportional to the ratio of  $NO_2$  to  $NO$  ( $O_3 \approx J_1 \cdot NO_2 / (k_{14} \cdot NO)$ ). Reactions that bias this  $NO_x$  ratio in favour of  $NO_2$  therefore result in higher ozone concentrations.

Two processes cause such a bias. The first is the reaction of  $NO$  with  $RO_2$  radicals to produce  $NO_2$ . These radicals ( $RO_2$ ,  $INO_2$ ,  $VRO_2$ ,  $MVN_2$ ,  $MRO_2$ , and  $MAN_2$ ) originate from isoprene's oxidation by  $OH$  and  $NO_3$ . The reaction rates for the first hour of the "high  $NO_x$  - high Isoprene" scenario have shown that 43% of the net (positive) rate of change of  $NO_2$  is due to production of  $NO_2$  via the  $RO_2$  reactions. The addition of isoprene causes the  $NO_2/NO$  ratio to move from 8.13 to 9.09.

This process is short-lived due to the rapid oxidation of isoprene and its product ketones within the first few hours of the simulation (example isoprene concentrations are given in Figure 3). This removes the source term for the  $RO_2$  radicals. The second increase in  $O_3$ , between hours 18 and 24 (6 am and noon) is due to the release of  $NO_2$  from the cycles of peroxyacetyl nitrate (PAN), MPAN, and

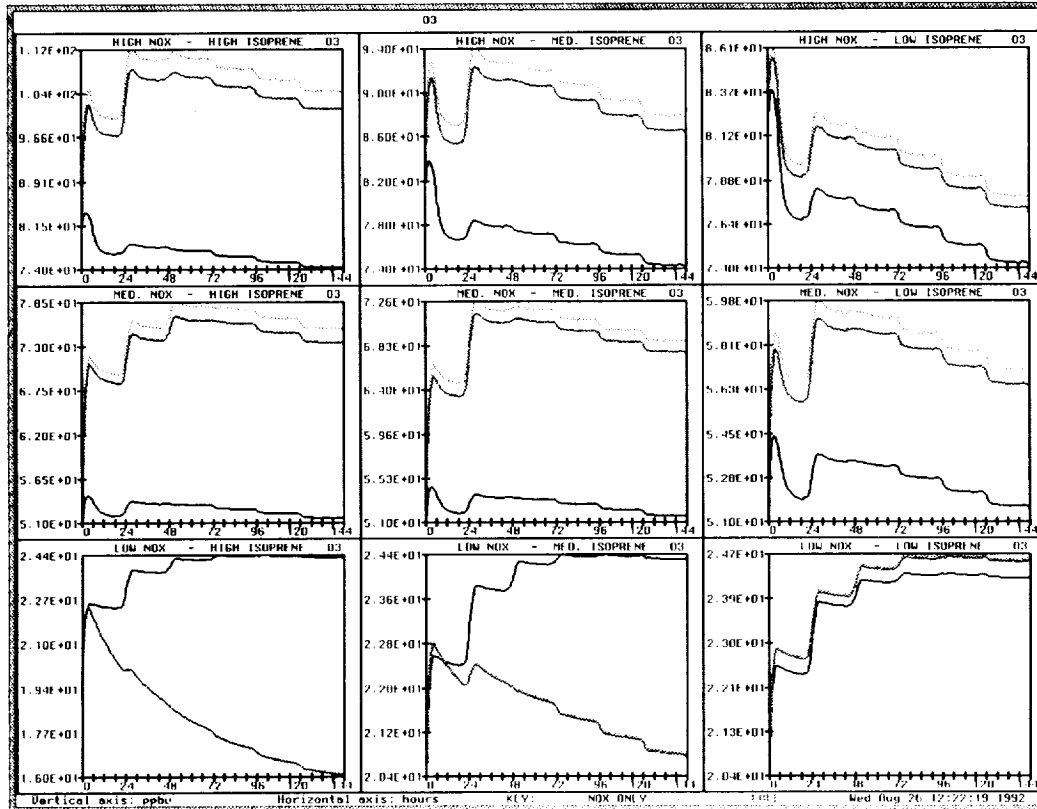


Figure 2.  $O_3$  Concentrations, Nine test cases. Light grey, dark grey, and black lines correspond to parameterization, full isoprene, and no isoprene values, respectively.

IPAN. These species have very similar reaction chemistry (hence their combination in the parameterization); production is via reaction of a peroxyacetyl radical with  $\text{NO}_2$ , and loss is via thermal dissociation of the compound back into  $\text{NO}_2$  and the radical. The colder temperatures during the night (hours 6 to 18) thus resulted in a buildup of the PAN-type species. The increase of temperatures on the dawn of the second day caused the release of  $\text{NO}_2$  stored during the night as PAN, MPAN and IPAN. These processes have a magnitude sufficient to account for the entire net rate of change of  $\text{NO}_2$  at 11:30 am on the second day.

The enhancement of  $\text{O}_3$  due to PAN-type compounds from isoprene oxidation has important implications with regards to ozone production far from the source region. For example,  $\text{NO}_x$  produced in a region of biomass burning (a high  $\text{NO}_x$ , high isoprene source region), if carried aloft a few kilometres (a temperature contrast equivalent to the day/night one used here) could be stored as PAN and related organic compounds. Later heating of the airmass far downwind from the source would result in strongly enhanced ozone. Such a mechanism may be responsible for the "Ozone high" in the troposphere over the South Atlantic, mentioned in other papers in these Proceedings.

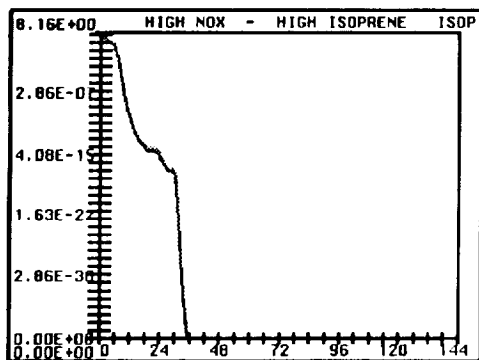


Figure 3. Isoprene Concentration, High  $\text{NO}_x$  - high isoprene. Light grey lines are parameterization results, dark grey lines are full isoprene mechanism.

The mechanism responsible for ozone depletion in the "low  $\text{NO}_x$ " simulations is that of removal by isoprene. Initial  $\text{NO}_x$  levels are sufficiently low so that the  $(\text{RO}_2 + \text{NO})$  ozone source fails to compensate for the loss of ozone due to isoprene oxidation. During the first nightfall, isoprene removal of ozone dominates the other loss terms by about two orders of magnitude. Thereafter the curve describing ozone concentrations closely follows that of isoprene, with a gradual decrease in both species.

Total lumped PAN's for high  $\text{NO}_x$  - high isoprene are given in Figure 4. Total PAN has increased by about an order of magnitude for the high and medium  $\text{NO}_x$  scenarios. The increase is smaller for the low  $\text{NO}_x$  case, and almost non-existent for the case of low- $\text{NO}_x$ , high-isoprene. The enhancement of total PAN's is due to the addition of the biogenic MPAN and IPAN to peroxyacetylnitrate. These species increase in concentration until the middle of the second day, when the concentrations of their ketone precursors have become depleted. The enhanced PAN cycle is one of the primary causes of the ozone enhancement noted above.

Methane, ethane and propane all have a "staircase" pattern of decreasing concentration (ethane is given as an example, Figure 5). The most rapid removal (steep parts of the steps) occurs during the day, when the oxidant, OH, is highest in concentration. The differences in the rate of alkane removal between isoprene and no isoprene cases thus reflect differences in OH concentrations. Ethane removal is enhanced by the addition of isoprene in the high and medium  $\text{NO}_x$  scenarios (ie. higher OH). In the low  $\text{NO}_x$  scenario, the addition of isoprene results in a decrease in the ethane removal rate (ie. lower OH). The OH values are a direct reflection of the  $\text{NO}_x$  changes discussed above. In the high  $\text{NO}_x$  - high isoprene case, daytime OH concentrations are enhanced by higher  $\text{O}_3$  and thus higher  $\text{O}(^1\text{D})$  values. In the low  $\text{NO}_x$  - high isoprene case, daytime OH is inhibited by removal by the as yet undepleted isoprene. At hour 24 for this scenario, the loss rate of OH due to isoprene alone is 4.2 times the combined loss rates due to CO and

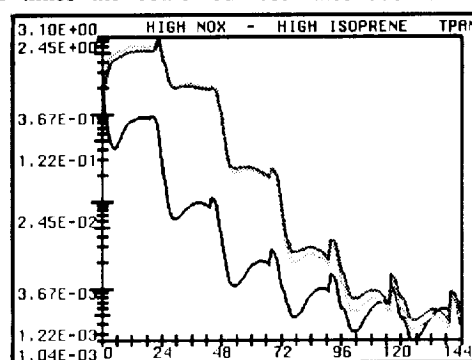


Figure 4. Total PAN (= PAN + MPAN + IPAN) Concentrations.

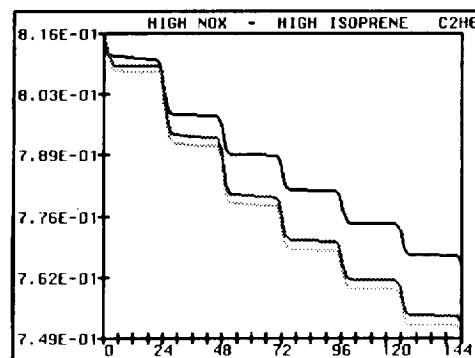


Figure 5. Ethane Concentrations.

$\text{CH}_4$  oxidation. When combined with the effects of its ketone products, methacrolein and methyl vinyl ketone, the isoprene-caused OH loss rate is 5.2 times the combined CO and  $\text{CH}_4$  loss rate. In regions where the isoprene concentration is high (eg. close to the source) it will be the main chemical determining OH concentrations.

Formic acid values are given in Figure 5 (again, high  $\text{NO}_x$  - high isoprene is used as an example). The production of formic acid is greatly enhanced by the introduction of isoprene for all test cases. This is due to the addition of the creige biradical CREA ( $\text{CH}_2\text{O}_2$ ) as a source of formaldehyde.

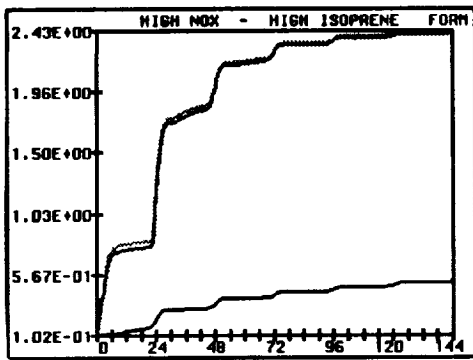


Figure 6. Formic Acid Concentrations.

**Conclusions:**

The isoprene parameterization derived in this work has been compared to a more detailed reaction mechanism, and has been found suitable for use in applications in which the number of chemicals are limited by computational memory and processing time. The parameterization uses 14 less species than the full mechanism, yet produces essentially the same results for the most important tropospheric gases.

The effect of isoprene on tropospheric chemistry depends on both the initial NO<sub>x</sub> and isoprene levels. Ozone was found to either increase or decrease in concentration depending on the initial NO<sub>x</sub> values. Increases were due to conversion of NO to NO<sub>2</sub>, with the causes of this conversion being RO<sub>2</sub> reactions with NO<sub>x</sub> and release of NO<sub>2</sub> from PAN-type compounds. Similar effects were shown for the other species studied. The lack of deposition or sources after the initial time showed that the injection of isoprene into an air mass can have a long term effect on the chemistry of that air mass, long after the precursor hydrocarbon has been totally oxidized.

Table 1: Initial Concentrations

Species	Concentration (ppbv)	Concentration (molecules cm <sup>-3</sup> )
NO <sub>2</sub>	0.1 / 3.0 / 8.0	0.25 / 7.4 / 20.0 (x10 <sup>10</sup> )
NO	0.02 / 1.0 / 1.8	0.05 / 2.5 / 4.4 (x10 <sup>10</sup> )
O <sub>3</sub>	20. / 50. / 80.	50. / 125. / 200. (x10 <sup>10</sup> )
NO <sub>x</sub>	0.04 ppbv	10 <sup>6</sup>
N <sub>2</sub> O <sub>5</sub>	0.04 ppbv	10 <sup>6</sup>
PAN	0.01 / 0.3 / 8.0	0.25 / 7.5 / 20. (x10 <sup>9</sup> )
HNO <sub>2</sub>	0.2	5.0 (x10 <sup>9</sup> )
HNO <sub>3</sub>	2.0	5.0 (x10 <sup>10</sup> )
HNO <sub>4</sub>	1.0 ppbv	2.5(x10 <sup>7</sup> )
CH <sub>4</sub>	1.67 ppmv	4.185 (x10 <sup>13</sup> )
HCHO	2.0	5.0 (x10 <sup>10</sup> )
MCHO	0.5	1.25 (x10 <sup>10</sup> )
MCO <sub>3</sub>	0.04 ppbv	10 <sup>6</sup>
MOOH	0.2	5.0 (x10 <sup>9</sup> )
MO <sub>2</sub>	0.04 ppbv	10 <sup>6</sup>
MO	0.04 ppbv	10 <sup>6</sup>
CO	200	5.0 (x10 <sup>12</sup> )
CO <sub>2</sub>	343 ppmv	8.575 (x10 <sup>13</sup> )
C <sub>2</sub> H <sub>6</sub>	0.8	2.0 (x10 <sup>10</sup> )
C <sub>3</sub> H <sub>8</sub>	0.2	5.0 (x10 <sup>10</sup> )
ETO <sub>2</sub>	0.04 ppbv	10 <sup>6</sup>
H <sub>2</sub> O <sub>2</sub>	0.5	1.25 (x10 <sup>10</sup> )
HO <sub>2</sub>	0.04 ppbv	10 <sup>6</sup>
OH	0.04 ppbv	10 <sup>6</sup>
FORM	0.1	2.5 (x10 <sup>10</sup> )
AHO <sub>2</sub>	0.04 ppbv	10 <sup>6</sup>
O <sup>(1)D</sup>	4.0 (x10 <sup>-10</sup> )	10 <sup>1</sup>
LOSS	4.0 (x10 <sup>-10</sup> )	10 <sup>1</sup>
H <sub>2</sub> O	1.5 %	3.829 (x10 <sup>17</sup> )
O <sub>2</sub>		5.131 (x10 <sup>18</sup> )
M		2.45 (x10 <sup>19</sup> )

**Full Isoprene Mechanism Initial Conditions:**

Species	Concentration (ppbv)	Concentration (molecules cm <sup>-3</sup> )
ISOP	0.5 / 3.1 / 8.2	1.23 / 7.50 / 20.0 (X10 <sup>10</sup> )
MACR	0.2	3.0 (x10 <sup>10</sup> )
MVK	0.2	3.0 (x10 <sup>10</sup> )
RIO <sub>2</sub>	0.04 ppbv	10 <sup>6</sup>
INO <sub>2</sub>	0.04 ppbv	10 <sup>6</sup>
MGGY	4 ppbv	10 <sup>6</sup>
IPAN	4 ppbv	10 <sup>6</sup>
MPAN	4 ppbv	10 <sup>6</sup>
HAC	0.01	2.5 (x10 <sup>9</sup> )
PYRU	0.04 ppbv	10 <sup>6</sup>
(all remaining species, same as PYRU)		(all remaining species: MAAC, VRO <sub>2</sub> , MAN <sub>2</sub> , MVN <sub>2</sub> , MRO <sub>2</sub> , IPN <sub>2</sub> , CREA, MVKO, MAOO, MCRG, MGLO, HACO, MAO <sub>2</sub> , and OZID, start at 10 <sup>6</sup> molecules cm <sup>-3</sup> ).

**Parameterization:**  
 ISOP, MACR, MVK, RIO<sub>2</sub>, INO<sub>2</sub>, MGGY, CREA are same as above. The radicals CREB, MBN<sub>2</sub>, and BRO<sub>2</sub> all start at 10<sup>6</sup> molecules cm<sup>-3</sup>. The lumped PAN has initial concentrations of 4.5x10<sup>9</sup>, 7.7x10<sup>9</sup>, and 2.02x10<sup>10</sup> molecules cm<sup>-3</sup> for low, medium and high NO<sub>x</sub> scenarios. The lumped MCHO concentration is 1.275x10<sup>9</sup> molecules cm<sup>-3</sup>.

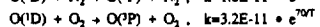
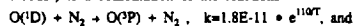
**Appendix I : Reaction Mechanisms**

No	Isoprene Reaction Mechanism	k <sub>1</sub>	k <sub>2</sub>	TYPE	SOURCE
1	NO <sub>2</sub> + hv → NO + O <sub>3</sub>			1	a
2	O <sub>3</sub> + hv → O <sup>(1)D</sup> + O <sub>2</sub>			1	a
3	H <sub>2</sub> O <sub>2</sub> + hv → 2 OH			1	a
4	HCHO + hv → H <sub>2</sub> + CO			1	a
5	HCHO + hv → 2 HO <sub>2</sub> + CO			1	a
6	MOOH + hv → MO + OH			1	a
7	N <sub>2</sub> O <sub>5</sub> + hv → NO <sub>2</sub> + NO <sub>3</sub>			1	a
8	HNO <sub>3</sub> + hv → OH + NO <sub>2</sub>			1	a
9	MCHO + hv → MO <sub>2</sub> + HO <sub>2</sub> + CO			1	a
10	NO <sub>x</sub> + hv → NO + O <sub>2</sub>			1	a
11	NO <sub>x</sub> + hv → NO <sub>2</sub> + O <sub>2</sub>			1	a
12	O <sup>(1)D</sup> + M → O <sub>3</sub> + M			special function	4 a
13	O <sup>(1)D</sup> + H <sub>2</sub> O → 2 OH	2.2E-10		3	a
14	O <sub>3</sub> + NO → NO <sub>2</sub> + O <sub>2</sub>	2.0E-12	1.4E+03	2	a
15	O <sub>3</sub> + OH → HO <sub>2</sub> + O <sub>2</sub>	1.6E-12	9.4E+02	2	a
16	O <sub>3</sub> + HO <sub>2</sub> → OH + 2 O <sub>2</sub>	1.1E-14	5.0E+02	2	a
17	O <sub>3</sub> + NO <sub>2</sub> → NO <sub>3</sub> + O <sub>2</sub>	1.2E-13	2.45E+03	2	a
18	OH + H <sub>2</sub> O <sub>2</sub> → HO <sub>2</sub> + H <sub>2</sub> O	2.9E-12	1.6E+02	2	a
19	OH + NO → HNO <sub>2</sub>			special function	4 b
20	OH + NO <sub>2</sub> → HNO <sub>3</sub>			special function	4 a
21	OH + HNO <sub>3</sub> → NO <sub>3</sub> + H <sub>2</sub> O			special function	4 a
22	OH + CO → HO <sub>2</sub> + CO <sub>2</sub>			special function	4 a
23	OH + CH <sub>4</sub> → MO <sub>2</sub> + H <sub>2</sub> O	2.3E-12	1.7E+03	2	a
24	OH + HCHO → HO <sub>2</sub> + CO + H <sub>2</sub> O	1.0E-11		3	a
25	OH + MOOH → MO <sub>2</sub> + H <sub>2</sub> O	3.8E-12	-2.0E+02	2	a
26	OH + MCHO → MCO <sub>3</sub> + H <sub>2</sub> O	6.9E-12	-2.5E+02	2	b
27	HO <sub>2</sub> + NO → NO <sub>2</sub> + OH	3.7E-12	-2.4E+02	2	a
28	HO <sub>2</sub> + OH → H <sub>2</sub> O + O <sub>2</sub>	4.8E-11	-2.5E+02	2	a
29	2 HO <sub>2</sub> → H <sub>2</sub> O <sub>2</sub> + O <sub>2</sub>	2.3E-13	-6.0E+02	2	a
30	HO <sub>2</sub> + MO <sub>2</sub> → MOOH + O <sub>2</sub>	3.3E-13	-8.0E+02	2	a
31	HO <sub>2</sub> + MCO <sub>3</sub> → LOSS	3.0E-12		3	b
32	HO <sub>2</sub> + NO <sub>2</sub> → HNO <sub>3</sub>			special function	4 b
33	NO <sub>2</sub> + NO <sub>2</sub> → N <sub>2</sub> O <sub>4</sub>			special function	4 a
34	NO <sub>2</sub> + NO <sub>3</sub> → NO + NO <sub>2</sub> + O <sub>2</sub>	2.5E-14	1.23E+03	2	b
35	N <sub>2</sub> O <sub>4</sub> → NO <sub>2</sub> + NO <sub>2</sub>			special function	4 b
36	NO <sub>2</sub> + NO → 2 NO <sub>2</sub>	8.0E-12	-2.5E+02	2	b
37	NO <sub>2</sub> + HCHO → HNO <sub>3</sub> + HO <sub>2</sub> + CO	3.2E-16		3	b
38	NO + MO <sub>2</sub> + NO <sub>2</sub> → MO	4.2E-12	-1.8E+02	2	b
39	NO <sub>2</sub> + MCO <sub>3</sub> + PAN	4.7E-12		3	b
40	NO + MCO <sub>3</sub> + MO <sub>2</sub> + CO <sub>2</sub> + NO <sub>2</sub>	4.2E-12	-1.8E+02	2	b
41	PAN + MCO <sub>3</sub> + NO <sub>2</sub>	1.95E+16	9.0E+02	2	a
42	MO + O <sub>2</sub> → HCHO + HO <sub>2</sub>	3.94E-14	9.0E+02	2	a
43	N <sub>2</sub> O <sub>5</sub> + H <sub>2</sub> O → 2 HNO <sub>3</sub>	1.3E-21		3	b
44	C <sub>2</sub> H <sub>6</sub> + OH → ETO <sub>2</sub> + H <sub>2</sub> O	1.7E-11	1.232E+03	2	b
45	ETO <sub>2</sub> + NO → MCHO + HO <sub>2</sub> + NO <sub>2</sub>	4.2E-12	-1.8E+02	2	b
46	2 ETO <sub>2</sub> → 1.6 MCHO + 1.2 HO <sub>2</sub>	5.0E-14		3	b
47	ETO <sub>2</sub> + HO <sub>2</sub> → LOSS	3.0E-12		3	b
48	C <sub>2</sub> H <sub>6</sub> + OH → ETO <sub>2</sub>	1.18E-11	6.79E+02	2	b
49	MCHO + NO <sub>2</sub> → MCO <sub>3</sub> + HNO <sub>3</sub>	1.4E-12	1.9E+03	2	a
50	HNO <sub>3</sub> + NO <sub>2</sub> → HO <sub>2</sub>			special function	4 b
51	HNO <sub>3</sub> + hv → NO + OH	0.205 x J(NO <sub>2</sub> )		1	b
52	HCHO + HO <sub>2</sub> → AHO <sub>2</sub>	1.0E-14		3	b
53	AHO <sub>2</sub> + NO → FORM + HO <sub>2</sub> + NO <sub>2</sub>	4.2E-12	-1.8E+02	2	b
54	AHO <sub>2</sub> + HO <sub>2</sub> → FORM + H <sub>2</sub> O + O <sub>2</sub>	2.0E-12		3	b
55	2 AHO <sub>2</sub> → 2 FORM + 2 HO <sub>2</sub> + 2 O <sub>2</sub>	1.0E-13		3	b
56	FORM + OH → HO <sub>2</sub> + H <sub>2</sub> O + CO <sub>2</sub>	3.2E-13		3	b

Comments:  
 (1) Photolysis rates from detailed model results at 0 km (see text).  
 (2) Temperature dependent rates, k = k<sub>0</sub> × exp(-k<sub>a</sub>/T), T = temp. in K.  
 (3) Constant rates.

(4) Special functions for given reactions:

(12) The reaction  $O(D) + M \rightarrow O_3 + M$  (the products are actually  $O_3(P) + M$ , but the conversion to  $O_3$  is assumed to be "instantaneous") is a combination of the reactions



If 80 % of M is  $N_2$  and 20 % is  $O_2$ , then the net reaction is



$$k_{net} = 1.44E-11 e^{110/T} + 6.4E-12 e^{70/T}$$

$$(19) \quad k = \left( \frac{A \cdot T^B \cdot [M]}{1 + \frac{A \cdot T^B \cdot [M]}{C \cdot T^D}} \right) \cdot 0.6 \left( 1 + \left( \log_{10} \frac{A \cdot T^B \cdot [M]}{C \cdot T^D} \right)^2 \right)^{-1}$$

$$A = 1.0E-22, B = -3.3, C = 9.0E-09, D = -1.0$$

$$(20) \quad k = \left( \frac{A \cdot [M]}{1 + \frac{A \cdot [M]}{B}} \right) \cdot 0.6 \left( 1 + \left( \log_{10} \frac{A \cdot [M]}{B} \right)^2 \right)^{-1}$$

$$A = 2.6E-30 \cdot (T/300)^{-3.2}, B = 2.4E-11 \cdot (T/300)^{-1.3}$$

$$(21) \quad k = A + \frac{C \cdot [M]}{1 + \frac{C \cdot [M]}{B}}, \quad A = 7.2E-15 \cdot \exp(785/T),$$

$$B = 4.1E-16 \cdot \exp(1440/T), C = 1.9E-33 \cdot \exp(725/T)$$

$$(22) \quad k = 1.50E-13 \cdot (1 + 0.6[M] \cdot T + 1.36E-16 / 1.013E+06)$$

$$(32) \quad k = \left( \frac{6.9E-33 \cdot [M] \cdot e^{1007/T}}{1 + 4.86E-12 \cdot [M]^{0.81}} \right)$$

(33) (same formula as reaction 20),

$$A = 2.2E-30 \cdot (T/300)^{-3.2}, B = 1.5E-12 \cdot (T/300)^{-0.5}$$

$$(35) \quad k = k_{35} \cdot 7.5E+26 \cdot (300/T)^{0.32} \cdot e^{-11000/T}$$

$$(50) \quad k = (4.9E-06 \cdot [M] \cdot \exp(-10015/T)) / (1 + 4.86E-12 \cdot [M]^{0.81})$$

In the above, [M] is the total number density in molecules  $cm^{-3}$ , and T is the temperature in degrees Kelvin.

Sources: (a) DeMore et al. 1990, (b) Lurmann et al. 1986

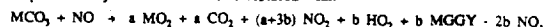
Parameterization Reactions:

57	ISOP	+ O <sub>3</sub>	+ 0.5 HCHO	+ 0.2 MVK	+ 0.30 MACR		
			+ 0.2 CREA	+ 0.06 HO <sub>2</sub>	+ 0.5 CREB	7.0E-15	1.9E+03 2
58	MVK	+ O <sub>3</sub>	+ 0.5 HCHO	+ 0.2 CREA	+ 0.21 HO <sub>2</sub>		
			+ 0.2 CREB	+ 0.15 MCHO	+ 0.5 MGGY		
			+ 0.15 MCO <sub>3</sub>			4.0E-15	2.0E+03 2
59	MACR	+ O <sub>3</sub>	+ 0.5 HCHO	+ 0.2 CREA	+ 0.21 HO <sub>2</sub>		
			+ 0.15 MO <sub>2</sub>	+ 0.5 MGGY		4.4E-15	2.5E+03 2
60	ISOP	+ OH	+ RIO <sub>2</sub>			1.5E-11	-5.0E+02 2
61	RIO <sub>2</sub>	+ NO	+ 0.9 NO <sub>2</sub>	+ 0.45 MVK	+ 0.45 MACR		
			+ 0.9 HO <sub>2</sub>	+ 0.9 HCHO		4.2E-12	-1.8E+02 2
62	INO <sub>2</sub>	+ NO	+ 2.0 NO <sub>2</sub>	+ HCHO	+ 0.5 MVK		
			+ 0.5 MACR			4.2E-12	-1.8E+02 2
63	INO <sub>2</sub>	+ NO <sub>2</sub>	+ LOSS			4.2E-13	-1.8E+02 2
64	ISOP	+ NO <sub>2</sub>	+ INO <sub>2</sub>			3.23E-13	3
65	CREA	+ H <sub>2</sub> O	+ FORM	+ H <sub>2</sub> O		4.0E-18	3
66	CREA	+ NO	+ HCHO	+ NO <sub>2</sub>		7.0E-12	3
67	CREA	+ NO <sub>2</sub>	+ HCHO	+ NO <sub>2</sub>		7.0E-13	3
68	CREB	+ H <sub>2</sub> O	+ LOSS	+ H <sub>2</sub> O		4.0E-18	3
69	CREB	+ NO	+ 0.33 MVK	+ 0.33 MACR	+ 0.33 MGGY		
			+ NO <sub>2</sub>			4.2E-12	-1.8E+02 2

70	CREB	+ NO <sub>2</sub>	+ 0.33 MVK	+ 0.33 MACR	+ 0.33 MGGY		
			+ NO <sub>2</sub>			4.2E-13	-1.8E+02 2
71	RIO <sub>2</sub>	+ HO <sub>2</sub>	+ LOSS			3.0E-12	3
72	INO <sub>2</sub>	+ HO <sub>2</sub>	+ LOSS			3.0E-12	3
73	MACR	+ NO <sub>2</sub>	+ MBN <sub>2</sub>			6.7E-15	3
74	MVK	+ NO <sub>2</sub>	+ MBN <sub>2</sub>			6.0E-14	3
75	MBN <sub>2</sub>	+ NO	+ 2.0 NO <sub>2</sub>	+ HCHO	+ 0.45 HO <sub>2</sub>		
			+ 0.45 MCO <sub>3</sub>	+ 0.55 MGGY		4.2E-12	-1.8E+02 2
76	MACR	+ NO <sub>2</sub>	+ MCO <sub>3</sub>	+ HNO <sub>3</sub>		3.3E-15	3
77	MGGY	+ MCO <sub>3</sub>	+ HO <sub>2</sub>			0.15	xJ(NO <sub>2</sub> )
78	MGGY	+ OH	+ MCO <sub>3</sub>			1.7E-11	3
79	MACR	+ OH	+ BRO <sub>2</sub>			3.86E-12	-5.0E+02 2
80	MACR	+ OH	+ MCO <sub>3</sub>			1.02E-11	
81	MVK	+ OH	+ BRO <sub>2</sub>			3.0E-12	-5.0E+02 2
82	BRO <sub>2</sub>	+ HO <sub>2</sub>	+ LOSS			3.0E-12	3
83	BRO <sub>2</sub>	+ NO	+ 0.9 NO <sub>2</sub>	+ 0.625 HO <sub>2</sub>	+ 0.625 HCHO		
			+ 0.625 MGGY	+ 0.275 MCO <sub>3</sub>	+ 0.275 MCHO	4.2E-12	-1.8E+02 2
84	MBN <sub>2</sub>	+ HO <sub>2</sub>	+ LOSS			3.0E-12	3

Comments:

(1) The first 56 reactions are those of the "No Isoprene" set, with the exception of reaction 40, which has been altered to reflect the lumped PAN cycle. Reaction 40 is replaced with:



$$b = \frac{k_{14}(MACR)(NO_2) + k_{15}(MACR)(OH)}{(k_{14}(NO_2) + k_{15}(OH))(MACR) + (k_{16}(NO_2) + k_{17}(OH))(MCHO) + 0.15 k_{18}(MVK)(O_3) + (0.45 k_{19}(MBN_2) + 0.275 k_{20}(BRO_2))(NO) + (k_{21} + k_{22})(MGGY)}$$

and  $a = 1.0 - b$ . In the parameterization, "MCO<sub>3</sub>", "MCHO", and "PAN" refer to the lumped peroxyacetyl radical, lumped higher aldehyde and lumped acetyl nitrate species, respectively.

(2) Temperature dependant rates:  $k = k_0 \exp(-k_a/T)$ , T = temperature in degrees K.

(3) Constant rates.

## REFERENCES

- DeMore, W.B., S.P. Sander, D.M. Golden, M.J. Molina, R.F. Hampson, M.J. Kurylo, C.J. Howard, A.R. Ravishankara, 1990: Chemical Kinetics and Photochemical Data for Use in Stratospheric Modelling. J.P.L. Publication 90-1, 1990, Jet Propulsion Laboratories, California Institute of Technology, Pasadena, California.
- Henderson, G.S, W.F.J. Evans, J.C. McConnell and E.M.J. Templeton, 1987: A Numerical Model for One Dimensional Simulation of Stratospheric Chemistry. Atmosphere - Ocean, 25, 427 - 459.
- Jacob, D.J., and S.C. Wofsy, 1988: Photochemistry of Biogenic Emissions Over the Amazon Forest. J. Geophys. Res., 93, D4, 1,477 - 1,486.
- Lurmann, F.W., A.C. Lloyd, and R. Atkinson, 1986: A Chemical Mechanism for Use in Long-Range Transport/Acid Deposition Computer Modeling. J. Geophys. Res., 91, D10, 10,905 - 10,936.
- Trainer, M., E.Y. Hsie, S.A. McKeen, R. Tallamraju, D.D. Parrish, F.C. Fehsenfeld, and S.C. Liu, 1987: Impact of Natural Hydrocarbons on Hydroxyl and Peroxy Radicals at a Remote Site. J. Geophys. Res., 92, D10, 11,879 - 11,894.